THE JOURNAL OF BIOLOGICAL CHEMISTRY VOL. 284, NO. 45, pp. 31006–31017, November 6, 2009

Ibuprofen Impairs Allosterically Peroxynitrite Isomerization by Ferric Human Serum Heme-Albumin*[S]

Received for publication, April 20, 2009, and in revised form, September 3, 2009 Published, JBC Papers in Press, September 3, 2009, DOI 10.1074/jbc.M109.010736

Paolo Ascenzi[‡§1,2], Alessandra di Masi[‡1], Massimo Coletta[¶‖], Chiara Ciaccio[¶], Gabriella Fanali[**], Francesco P. Nicoletti[‡‡], Giulietta Smulevich[‖‡‡], and Mauro Fasano[**]

From the [‡]Department of Biology and Interdepartmental Laboratory for Electron Microscopy, University Roma Tre, I-00146 Roma, Italy, the [§]National Institute for Infectious Diseases I.R.C.C.S. "Lazzaro Spallanzani," I-00149 Roma, Italy, the [¶]Department of Experimental Medicine and Biochemical Sciences, University of Roma "Tor Vergata," I-00133 Roma, Italy, the [‖]Interuniversity Consortium for Research on the Chemistry of Metals in Biological Systems, I-70126 Bari, Italy, the [**]Department of Structural and Functional Biology and Center of Neuroscience, University of Insubria, I-21052 Busto Arsizio (VA), Italy, and the [‡‡]Department of Chemistry, University of Firenze, I-50019 Sesto Fiorentino (FI), Italy

Human serum albumin (HSA) participates in heme scavenging; in turn, heme endows HSA with myoglobin-like reactivity and spectroscopic properties. Here, the allosteric effect of ibuprofen on peroxynitrite isomerization to NO_3^- catalyzed by ferric human serum heme-albumin (HSA-heme-Fe(III)) is reported. Data were obtained at 22.0 °C. HSA-heme-Fe(III) catalyzes peroxynitrite isomerization in the absence and presence of CO_2; the values of the second order catalytic rate constant (k_{on}) are 4.1×10^5 and 4.5×10^5 M^{-1} s^{-1}, respectively. Moreover, HSA-heme-Fe(III) prevents peroxynitrite-mediated nitration of free added L-tyrosine. The pH dependence of k_{on} ($pK_a = 6.9$) suggests that peroxynitrous acid reacts preferentially with the heme-Fe(III) atom, in the absence and presence of CO_2. The HSA-heme-Fe(III)-catalyzed isomerization of peroxynitrite has been ascribed to the reactive pentacoordinated heme-Fe(III) atom. In the absence and presence of CO_2, ibuprofen impairs dose-dependently peroxynitrite isomerization by HSA-heme-Fe(III) and facilitates the nitration of free added L-tyrosine; the value of the dissociation equilibrium constant for ibuprofen binding to HSA-heme-Fe(III) (L) ranges between 7.7×10^{-4} and 9.7×10^{-4} M. Under conditions where [ibuprofen] is $\gg L$, the kinetics of HSA-heme-Fe(III)-catalyzed isomerization of peroxynitrite is superimposable to that obtained in the absence of HSA-heme-Fe(III) or in the presence of non-catalytic HSA-heme-Fe(III)-cyanide complex and HSA. Ibuprofen binding impairs allosterically peroxynitrite isomerization by HSA-heme-Fe(III), inducing the hexacoordination of the heme-Fe(III) atom. These results represent the first evidence for peroxynitrite isomerization by HSA-heme-Fe(III), highlighting the allosteric modulation of HSA-heme-Fe(III) reactivity by heterotropic interaction(s), and outlining the role of drugs in modulating HSA functions. The present results could be relevant for the drug-dependent protective role of HSA-heme-Fe(III) *in vivo*.

Human serum albumin (HSA),[3] the most abundant protein in plasma (reaching a blood concentration of about 7.0×10^{-4} M), is characterized by an extraordinary ligand binding capacity, providing a depot and carrier for many compounds. HSA affects the pharmacokinetics of many drugs; holds some ligands in a strained orientation, providing their metabolic modification; renders potential toxins harmless, transporting them to disposal sites; accounts for most of the antioxidant capacity of human serum; and displays (pseudo)enzymatic properties (1–14).

HSA is a single non-glycosylated all-α-chain protein constituted by 585 amino acids, containing three homologous domains (labeled I, II, and III). Each domain is made up by two separate helical subdomains (named A and B), connected by random coils. Terminal regions of sequential domains contribute to the formation of interdomain helices linking domain IB to IIA and domain IIB to IIIA, respectively (Fig. 1) (2, 3, 5, 7, 11, 13–25).

The structural organization of HSA provides a variety of ligand binding sites (Fig. 1). According to Sudlow's nomenclature, bulky heterocyclic anions bind preferentially to Sudlow's site I (located in subdomain IIA), whereas Sudlow's site II (located in subdomain IIIA) is preferred by aromatic carboxylates with an extended conformation (Fig. 1). Warfarin and ibuprofen are considered as stereotype ligands for Sudlow's site I and II, respectively (1–3, 5, 12, 14, 16, 20, 26–30).

HSA is able to bind seven equivalents of long-chain fatty acids (FAs) at multiple binding sites (labeled *FA1–FA7* in Fig. 1) with different affinity (24, 31). In particular, FA1 is located within the IB subdomain, contacting the IB-IIA polypeptide linker and the long IB-IIA transdomain helix; FA2 is located at the interface between subdomains IA, IB, and IIA; FA3 and FA4 together contribute to Sudlow's site II (*i.e.* the ibuprofen site in subdomain IIIA); FA5 is located within subdomain IIIB with the ligand polar head oriented toward subdomain IIIA; FA6 is at the interface between subdomains IIA and IIB; FA7 corresponds to Sudlow's site I (*i.e.* the warfarin binding site in subdomain IIA). FA2 and FA6 clefts appear to be the secondary binding sites of ibuprofen (1, 3, 12, 14, 16, 18–20, 32–35).

* This work was supported in part by grants from the Ministry for Health of Italy (National Institute for Infectious Diseases I.R.C.C.S. "Lazzaro Spallanzani," Roma, Italy, Ricerca Corrente 2008) (to P. A.) and the Italian Ministry of University and Research (COFIN 2007SFZXZ7002) (to M. C.).

[S] The on-line version of this article (available at http://www.jbc.org) contains supplemental Tables S1 and S2 and Figs. S1 and S2.

[1] Both authors contributed equally to this work.

[2] To whom correspondence should be addressed: Dept. of Biology, University Roma Tre, Viale Guglielmo Marconi 446, I-00146 Roma, Italy. Tel.: 39-06-5733-3494; Fax: 39-06-5733-6321; E-mail: ascenzi@uniroma3.it.

[3] The abbreviations used are: HSA, human serum albumin; FA, fatty acid; Hb, hemoglobin; HSA-heme, human serum heme-albumin; HSA-heme-Fe(III)-CN, HSA-heme-Fe(III)-cyanide complex; HSA-heme-Fe(II)-NO, ferrous nitrosylated HSA; HSA-heme-Fe(III), ferric HSA-heme; Mb, myoglobin; HPLC, high pressure liquid chromatography.

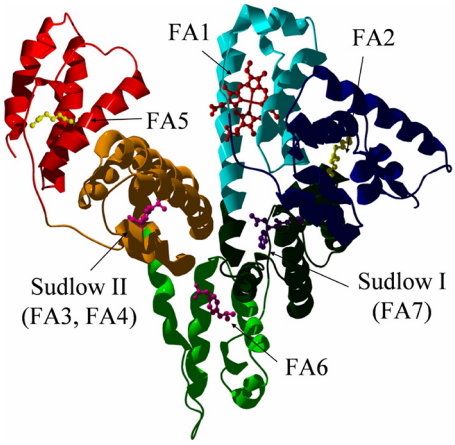

FIGURE 1. **HSA structure.** The six subdomains of HSA are *colored* as follows. *Blue*, subdomain IA; *cyan*, subdomain IB; *dark green*, subdomain IIA; *light green*, subdomain IIB; *orange*, subdomain IIIA; *red*, subdomain IIIB. The heme (*red*) fits the primary cleft in subdomain IB, corresponding to FA1. Sudlow's site I (in subdomain IIA, corresponding to FA7) is occupied by warfarin (*purple*). Sudlow's site II (in subdomain IIIA, corresponding to FA3-FA4) and FA6 (in subdomain IIB) are occupied by ibuprofen (*magenta*). Sites FA2 (at the I-IIA interface) and FA5 (in subdomain IIIB) are occupied by myristate (*yellow*). Atomic coordinates were taken from Protein Data Bank entries 1O9X (23), 1H9Z (20), and 2BXG (12).

The FA1 binding site has been shown to be the primary binding site for heme, bilirubin, and fusidic acid, an antibiotic that competitively displaces bilirubin from HSA (14, 21, 23). There is increasing evidence that FA1 has evolved to selectively bind heme-Fe(III) with high affinity ($K_d = 1.0 \times 10^{-8}$ M) (21, 23–25, 36, 37). The tetrapyrrole ring is arranged in a D-shaped cavity limited by Tyr^{138} and Tyr^{161} residues that provide $\pi-\pi$ stacking interactions with the porphyrin and supply a donor oxygen (from Tyr^{161}) for the heme-Fe(III) atom. Heme-Fe(III) is secured to HSA by the long IA-IB connecting loop (21, 23–25, 36–38). In turn, heme endows HSA with myoglobin (Mb)-like reactivity and spectroscopic properties (11, 21, 23, 28, 30, 36–55).

Both heme-Fe(III) binding to HSA and HSA-heme-Fe(II) reactivity are modulated allosterically, such that HSA-heme could be considered as a prototype monomeric allosteric macromolecule (21, 23–25, 30, 36–38, 45, 48, 52, 56). Indeed, the affinity of the heme-Fe(III) for HSA decreases by about 1 order of magnitude upon drug (*e.g.* warfarin) binding; on the other hand, heme-Fe(III) binding to HSA decreases the drug affinity by the same extent (57). Further, heme-Fe(III) inhibits ligand binding to Sudlow's site I by stabilizing the basic state of HSA, whereas ligand association to Sudlow's site I impairs HSA-heme-Fe(III) formation by stabilizing the neutral state of HSA (21, 23–25, 30, 36, 52, 56). Moreover, heme-Fe(III) modulates competitively and allosterically FA binding to HSA, since myristate binding to all FA sites competes with heme-Fe(III) binding to FA1 and at the same time induces the neutral to basic transition, facilitating heme-Fe(III) binding (5, 13, 23, 25, 37). In addition, abacavir and warfarin have been reported to modulate allosterically peroxynitrite-mediated oxidation of ferrous nitrosylated HSA (HSA-heme-Fe(II)-NO) (50) and NO dissociation from HSA-heme-Fe(II)-NO (51).

Here, ibuprofen, the prototype ligand of Sudlow's site II (1, 3, 26, 58), is reported to impair peroxynitrite[4] isomerization to NO_3^- by HSA-heme-Fe(III), in the absence and presence of CO_2. In the absence of ibuprofen, the pentacoordinated HSA-heme-Fe(III) form catalyzes peroxynitrite isomerization to NO_3^-, preventing the nitration of free added L-tyrosine. In contrast, ibuprofen induces hexacoordination of the heme-Fe(III) atom of HSA-heme-Fe(III), impairing allosterically peroxynitrite isomerization by HSA-heme-Fe(III) and allowing the nitration of free added L-tyrosine. These results represent the first evidence for a drug-dependent peroxynitrite scavenging by HSA-heme-Fe(III), a condition possibly occurring in patients with various hemolytic diseases (59).

EXPERIMENTAL PROCEDURES

Materials

Hemin (Fe(III)-protoporphyrin IX) chloride was purchased from Sigma. The heme stock solution (5.0×10^{-3} M) was prepared by dissolving heme-Fe(III) in 1.0×10^{-2} M NaOH (60). The heme-Fe(III) concentration was determined spectrophotometrically at 535 nm, after converting heme-Fe(III) to the heme-Fe(III)-bisimidazolate derivative by adding 1.0 M imidazole, in SDS micelles ($\epsilon_{535\ nm} = 14.5 \times 10^3\ M^{-1}\ cm^{-1}$) (61).

HSA (≥96%, essentially fatty acid-free) was obtained from Sigma. To remove hydrophobic ligands, HSA was dissolved in water, acidified to pH 3.5 with acetic acid, and treated for 2 h with activated charcoal at room temperature. After charcoal removal by centrifugation, the pH was brought to 7.0 with aqueous ammonia (62). The HSA concentration was determined spectrophotometrically at 280 nm ($\epsilon_{280\ nm} = 38.2 \times 10^3\ M^{-1}\ cm^{-1}$) (60). The HSA stock solution (2.0×10^{-4} M) was prepared by diluting the hydrophobic ligand-free HSA solution with the 2.0×10^{-2} M sodium phosphate buffer, at pH 7.2. The HSA-heme-Fe(III) stock solution (2.0×10^{-4} M) was prepared by adding a 0.9-fold molar defect of the heme-Fe(III) stock solution to the HSA solution (2.0×10^{-2} M sodium phosphate buffer, pH 7.2) (30, 37, 42, 44, 50, 54, 55, 60, 63). The HSA and HSA-heme(III) stock solutions were diluted in the 2.0×10^{-1} M sodium phosphate buffer at the desired pH value (ranging between 6.2 and 8.1) and concentration (ranging between 1.0×10^{-5} and 1.0×10^{-4} M).

Peroxynitrite was synthesized from KO_2 and •NO and from HNO_2 and H_2O_2 and stored in small aliquots at −80.0 °C (64, 65). The peroxynitrite stock solution (2.0×10^{-3} M) was diluted immediately before use with degassed 5.0×10^{-2} M NaOH to reach the desired concentration (50, 66–69). Nitrate and nitrite contaminations were in the range of 0–7% and 8–19% of the peroxynitrite concentration, respectively (see "Methods"). The concentration of peroxynitrite was determined spectrophotometrically prior to each experiment by measuring the absorbance at 302 nm ($\epsilon_{302\ nm} = 1.705 \times 10^3\ M^{-1}\ cm^{-1}$) (64, 65).

Experiments in the presence of CO_2, between pH 6.2 and 8.1, were carried out by adding to the protein solutions the required amount of a 5.0×10^{-1} M $NaHCO_3$ solution. After the addition

[4] The recommended IUPAC nomenclature for peroxynitrite is oxoperoxonitrate(1-), and the recommended nomenclature for peroxynitrous acid is hydrogen oxoperoxonitrate. The term "peroxynitrite" is used here to refer generically to both $ONOO^-$ and its conjugate acid ONOOH (67, 70, 72).

of bicarbonate, the protein solutions were allowed to equilibrate for at least 5 min. For the experiments carried out in the absence of CO_2, all solutions were thoroughly degassed and kept under nitrogen or helium (50, 66–69).

Experiments in the presence of cyanide at pH 7.2 were carried out by adding 2.0×10^{-1} M cyanide to the HSA-heme(III) and peroxynitrite/ibuprofen/L-tyrosine solutions, in the absence and presence of CO_2. This cyanide concentration allowed to obtain more than 90% of HSA-heme-Fe(III)-cyanide complex (HSA-heme-Fe(III)-CN) (43, 52).

Ibuprofen was obtained from Sigma. The ibuprofen stock solution (1.0×10^{-2} M) was prepared by dissolving the drug in 2.0×10^{-2} M phosphate buffer at pH 7.2 (30). The final ibuprofen concentration ranged between 5.0×10^{-5} and 1.0×10^{-2} M.

L-Tyrosine and nitro-L-tyrosine were obtained from Sigma. L-Tyrosine and nitro-L-tyrosine were dissolved in 1.0×10^{-1} M phosphate buffer, at pH 7.2; the final L-tyrosine concentration was 1.0×10^{-4} M (67, 70).

All of the other chemicals were obtained from Sigma and Merck. All products were of analytical or reagent grade and were used without further purification.

Methods

The kinetics of peroxynitrite isomerization in the absence and presence of HSA-heme-Fe(III), HSA-heme-Fe(III)-CN, HSA, CO_2, ibuprofen, and L-tyrosine was recorded with the SMF-20 and SMF-400 rapid mixing stopped-flow apparatus (Bio-Logic SAS, Claix, France). The light path of the observation cuvette was 10 mm, and the dead time was 1.4 ms. The kinetics was monitored at 302 nm, the characteristic absorbance maximum of peroxynitrite (64, 65). Kinetic data were obtained in the absence and presence of CO_2 (final concentration, 1.2×10^{-3} M) and ibuprofen (final concentration, 5.0×10^{-5} to 1.0×10^{-2} M) by rapid mixing the protein solution (final concentration, 5.0×10^{-6} to 5.0×10^{-5} M) or the buffer solution (1.0×10^{-1} M phosphate buffer) with the peroxynitrite solution (final concentration, 2.5×10^{-5} to 2.5×10^{-4} M). The kinetics was obtained at 22.0 °C and between pH 6.2 and 8.1 (1.0×10^{-1} M phosphate buffer); the pH was always measured at the end of the reaction. No gaseous phase was present.

The kinetics of peroxynitrite isomerization in the absence and presence of HSA-heme-Fe(III) was analyzed in the framework of the minimum reaction Schemes 1 and 2, respectively (67, 70),

$$\mathrm{HOONO} \xrightarrow{k_0} \mathrm{NO_3^-} + \mathrm{H^+}$$

SCHEME 1

$$\mathrm{HSA\text{-}heme\text{-}Fe(III)} + \mathrm{HOONO} \xrightarrow{k_{on}} \mathrm{HSA\text{-}heme\text{-}Fe(III)\text{-}OONO} \xrightarrow{fast} \mathrm{HSA\text{-}heme\text{-}Fe(III)} + \mathrm{NO_3^-} + \mathrm{H^+}$$

SCHEME 2

Values of the first-order rate constant for peroxynitrite isomerization in the presence of HSA-heme-Fe(III)-CN, HSA, and 1.0×10^{-1} M phosphate buffer (*i.e.* k_0 or k_0^i in the absence and presence of ibuprofen, respectively) and of the pseudo-first-order rate constant for HSA-heme-Fe(III)-mediated peroxynitrite isomerization (*i.e.* k_{obs} or k_{obs}^i in the absence and presence of ibuprofen, respectively) have been determined, in the absence and presence of CO_2, between pH 6.2 and 8.1 at 22.0 °C, from the analysis of the time-dependent absorbance decrease at 302 nm, according to Equation 1 (67, 69–74),

$$[\text{peroxynitrite}]_t = [\text{peroxynitrite}]_i \times e^{-k \times t} \qquad \text{(Eq. 1)}$$

where k is k_0 or k_{obs} in the absence of ibuprofen and k_0^i or k_{obs}^i in the presence of ibuprofen.

Values of the second-order rate constant for HSA-heme-Fe(III)-mediated peroxynitrite isomerization (*i.e.* k_{on} or k_{on}^i in the absence and presence of ibuprofen, respectively) have been determined, in the absence and presence of CO_2, between pH 6.2 and 8.1 at 22.0 °C, from the linear dependence of k_{obs} or k_{obs}^i on the HSA-heme-Fe(III) concentration according to Equations 2 and 3 (67, 70, 71, 73),

$$k_{obs} = k_{on} \times [\text{HSA-heme-Fe(III)}] + k_0 \qquad \text{(Eq. 2)}$$

$$k_{obs}^i = k_{on}^i \times [\text{HSA-heme-Fe(III)}] + k_0^i \qquad \text{(Eq. 3)}$$

The pH dependence of k_0 and k_{on} for peroxynitrite isomerization in the absence and presence of HSA-heme-Fe(III) allows us to obtain, in the absence of ibuprofen and both in the absence and presence of CO_2, at 22.0 °C, the values of pK_a, $k_{lim(top)}$ and $k_{lim(bottom)}$ (67, 70–72) according to Equation 4,

$$k = ((k_{lim(top)} \times 10^{-pH})/(10^{-pH} + 10^{-pK_a})) \qquad \text{(Eq. 4)}$$

where k is k_0 or k_{on}, and $k_{lim(top)}$ represents the top asymptotic value of k under conditions where pH $\ll pK_a$, and Equation 5,

$$k = (((k_{lim(top)} - k_{lim(bottom)}) \times 10^{-pH})/(10^{-pH} + 10^{-pK_a})) + k_{lim(bottom)} \qquad \text{(Eq. 5)}$$

where k is k_0 or k_{on}, and $k_{lim(top)}$ and $k_{lim(bottom)}$ represent the asymptotic values of k under conditions where pH $\ll pK_a$ or pH $\gg pK_a$, respectively.

The value of the dissociation equilibrium constant for ibuprofen binding to HSA-heme-Fe(III) (L) was determined, at pH 7.2, from the dependence of k_{on}^i on the ibuprofen concentration (ranging between 5.0×10^{-5} and 1.0×10^{-2} M). The effect of ibuprofen concentration on k_{on}^i was analyzed according to Equation 6 (30, 51, 71),

$$k_{on}^i = k_{on(top)}^i - ((k_{on(top)}^i \times [\text{ibuprofen}])/(L + [\text{ibuprofen}])) \qquad \text{(Eq. 6)}$$

where $k_{on(top)}^i$ represents the asymptotic value of k_{on}^i under conditions where [ibuprofen] = 0 (*i.e.* $k_{on(top)}^i = k_{on}$).

NO_2^- and NO_3^- analysis was carried out spectrophotometrically at 543 nm by using the Griess reagent and VCl3 to catalyze the conversion of NO_3^- to NO_2^-, as described previously (70, 75, 76). Calibration curves were obtained by measuring 4–8 standard sodium nitrite and sodium nitrate solutions in 1.0×10^{-1} M

phosphate buffer, pH 7.2, and 22.0 °C. The samples were prepared by mixing 500 μl of a HSA-heme-Fe(III) solution (initial concentration, 1.0×10^{-4} M in 2.0×10^{-1} M phosphate buffer, pH 7.2) with 500 μl of a peroxynitrite solution (initial concentration, 4.0×10^{-4} M in 1.0×10^{-2} M NaOH) while vortexing, at 22.0 °C, in the absence and presence of CO_2 (1.2×10^{-3} M) and ibuprofen (2.5×10^{-3} M). The reaction mixture was analyzed within ~10 min. At least four separate experiments were carried out.

The reaction of peroxynitrite with free L-tyrosine was carried out at pH 7.2 and 22.0 °C by adding 0.2 ml of an alkaline (1.0×10^{-2} M NaOH) ice-cooled solution of peroxynitrite (2.0×10^{-3} M) to 1.8 ml of a buffered (1.0×10^{-1} M phosphate buffer) solution of L-tyrosine (final concentration, 1.0×10^{-4} M) in the absence and presence of HSA-heme-Fe(III), HSA-heme-Fe(III)-CN, HSA (final concentration, 5.0×10^{-6} to 5.0×10^{-5} M), ibuprofen (final concentration, 2.0×10^{-4} to 5.0×10^{-3} M), and CO_2 (final concentration, 1.2×10^{-3} M), as previously reported (67, 70).

The amount of nitro-L-tyrosine was determined by HPLC, as reported previously (67, 70). The chromatographic system consisted of a Waters 600 pump and a Waters autosampler 717 PLUS equipped with a spectrophotometric UV-visible dual wavelength system, Waters 2487 (Waters, Milford, MA). Nitro-L-tyrosine separation was performed at 24.0 °C on the Grace Vydac 218TP54 Protein&Peptide C18 column (250 × 4.6 mm) equipped with a Grace Vydac guard cartridge filled with the same packing material (Grace Vydac, Columbia, MD). The mobile phase was composed of solutions A (0.07% trifluoroacetic acid in H_2O) and B (0.07% trifluoroacetic acid in acetonitrile). Both solutions were degassed by purging with helium. The injection volume was 20 μl. Nitro-L-tyrosine was eluted (7.48 ± 0.05 min after injection) by keeping the amount of solvent B constant (5%) in the first 2 min and then by using an increasing linear gradient of B from 5 to 10% between 2 and 10 min and from 10 to 80% between 10 and 15 min. Nitro-L-tyrosine was detected at 220, 280, 350, and 400 nm. Nitro-L-tyrosine was quantified by measuring a calibration curve of seven nitro-L-tyrosine standard solutions. The Millenium software (Waters) was used to pilot the HPLC instrument and to process the data (*i.e.* area integration, calculation, and plotting of chromatograms) throughout the method validation and sample analysis.

The value of the dissociation equilibrium constant for ibuprofen binding to HSA-heme-Fe(III) (L) was determined, at pH 7.2 and 22.0 °C, from the dependence of the relative yield of nitro-L-tyrosine formed from the reaction of peroxynitrite with free L-tyrosine (Y) on the drug concentration ([ibuprofen], ranging between 2.0×10^{-4} and 5.0×10^{-3} M). The effect of the ibuprofen concentration on Y was analyzed according to Equation 7 (30, 51, 71),

$$Y = (((100 - R) \times [\text{ibuprofen}])/(L + [\text{ibuprofen}])) + R \quad \text{(Eq. 7)}$$

where R corresponds to Y in the absence of ibuprofen.

The value of the dissociation equilibrium constant for ibuprofen binding to HSA-heme-Fe(III) (L) was also obtained spectrophotometrically at 404 nm (by a Cary 50 Bio spectrophotometer; Varian Inc., Palo Alto, CA), using an optical cell with 1.0-cm path length, at 22.0 °C. Small aliquots of the 1.2×10^{-2} M heme-Fe(III) and 1.0×10^{-3} M HSA solutions were diluted in the optical cell in 1.0×10^{-1} M phosphate buffer, 10% DMSO, pH 7.0, to a final HSA-heme-Fe(III) concentration of 1.0×10^{-5} M. Then small aliquots of the 1.0×10^{-3} M ibuprofen solution were added to the HSA-heme-Fe(III) solution, and the absorbance spectra were recorded after incubation for a few minutes after each addition. Ibuprofen binding to HSA-heme-Fe(III) was analyzed by plotting the Soret band absorbance change (ΔA) as a function of the ibuprofen concentration. Data were analyzed according to Equation 8 (30, 51, 71),

$$\Delta A = \Delta A_{max} \times [\text{ibuprofen}]/(L + [\text{ibuprofen}]) \quad \text{(Eq. 8)}$$

where ΔA_{max} is the absorbance change at saturating ibuprofen concentration.

Kinetic and thermodynamic data were analyzed using the MatLab program (The Math Works Inc., Natick, MA). The results are given as mean values of at least four experiments ± S.D.

RESULTS

HSA-Heme(III) Catalyzes Peroxynitrite Isomerization—The kinetics of peroxynitrite isomerization, both in the absence and presence of HSA-heme-Fe(III), HSA-heme-Fe(III)-CN, HSA, and CO_2, was recorded by a single-wavelength stopped-flow apparatus. Under all of the experimental conditions, a decrease of the absorbance at 302 nm was observed, as previously reported (67, 69, 70, 72–74). The kinetics of peroxynitrite isomerization was fitted to a single-exponential decay for more than 97% of its course (supplemental Fig. S1). According to the literature (67, 70), this indicates that no intermediate species (*e.g.* HSA-heme-Fe(III)-OONO; see Scheme 2) accumulate(s) in the course of peroxynitrite isomerization. In particular, the formation of the transient HSA-heme-Fe(III)-OONO species represents the rate-limiting step in catalysis, the conversion of the HSA-heme-Fe(III)-OONO complex to HSA-heme-Fe(III) and NO_3^- being faster by at least 1 order of magnitude.

In the absence of CO_2, the observed rate constant for HSA-heme-Fe(III)-catalyzed isomerization of peroxynitrite (k_{obs}) increases linearly with the HSA-heme-Fe(III) concentration over the whole pH range explored (Fig. 2*A*). The analysis of data reported in Fig. 2*A*, according to Equation 2, allowed the determination of values of the first-order rate constant for peroxynitrite isomerization in the absence of HSA-heme-Fe(III) (k_0; corresponding to the y intercept of the linear plots) and of the second-order rate constant for peroxynitrite isomerization by HSA-heme-Fe(III) (k_{on}; corresponding to the slope of the linear plots). Values of k_0 for peroxynitrite isomerization in the absence of HSA-heme-Fe(III) (Table 1) are in good agreement with those obtained in the presence of HSA-heme-Fe(III)-CN and HSA (Fig. 2*B*) and reported in the literature (67, 70, 72, 74).

Because of the physiological relevance attributed to the reaction between CO_2 and peroxynitrite (79, 74, 77–79), the effect of the physiological concentration of CO_2 on peroxynitrite isomerization by HSA-heme-Fe(III), HSA-heme-Fe(III)-CN,

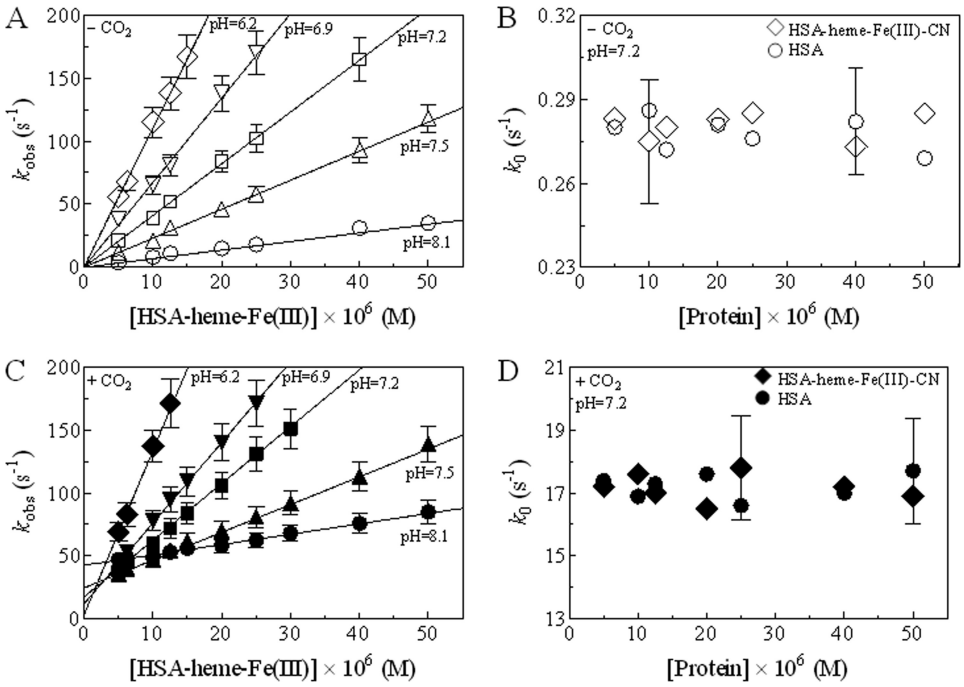

FIGURE 2. **Dependence of the (pseudo-)first-order rate constant for peroxynitrite isomerization on the HSA-heme-Fe(III) (k_{obs}; *A* and *C*), HSA-heme-Fe(III)-CN (k_0; *B* and *D*), and HSA (k_0; *B* and *D*) concentration, in the absence (*A* and *B*) and presence (*C* and *D*) of CO_2 at 22.0 °C.** The peroxynitrite concentration was 2.5×10^{-4} M. The CO_2 concentration was 1.2×10^{-3} M. The *continuous lines* in *A* and *C* were calculated according to Equation 2 with values of k_0 and k_{on} given in Table 1. Where not shown, the S.D. value is smaller than the *symbol* in *A* and *C*. For clarity, the S.D. is shown for two k_0 values in *B* and *D*.

TABLE 1

pH dependence of k_0 and k_{on} values for peroxynitrite isomerization in the absence and presence of HSA-heme-Fe(III) and CO_2, at 22.0 °C

1.0×10^{-1} M sodium phosphate buffer was used. The CO_2 concentration was 1.2×10^{-3} M. In italic type are shown the values of k_0 for peroxynitrite isomerization obtained in the absence of HSA-heme-Fe(III). In normal type are shown values of k_0 for HSA-heme-Fe(III)-catalyzed peroxynitrite isomerization.

pH	k_0		k_{on}	
	Without CO_2	With CO_2	Without CO_2	With CO_2
	s^{-1}		$M^{-1} s^{-1}$	
6.2	*0.67*	*4.1*		
	0.69	3.9	1.1×10^6	1.3×10^6
6.4	*0.64*	*6.2*		
	0.62	6.1	9.8×10^5	9.6×10^5
6.7	*0.43*	*8.9*		
	0.48	9.1	7.9×10^5	8.1×10^5
6.9	*0.35*	*11.9*		
	0.38	12.3	6.7×10^5	6.4×10^5
7.2	*0.28*	*17.4*		
	0.26	17.8	4.1×10^5	4.5×10^5
7.5	*0.11*	*25.3*		
	0.14	24.9	2.3×10^5	2.2×10^5
7.8	*0.086*	*32.9*		
	0.078	33.5	1.3×10^5	1.5×10^5
8.1	*0.046*	*43.7*		
	0.041	42.8	6.8×10^4	8.2×10^4

and HSA has been investigated. As shown in Fig. 2*C*, HSA-heme-Fe(III) catalyzes the isomerization of peroxynitrite in a concentration-dependent linear fashion. The analysis of data reported in Fig. 2*C*, according to Equation 2, allowed the determination of values of the first-order rate constant for peroxynitrite isomerization in the absence of HSA-heme-Fe(III) (k_0; corresponding to the *y* intercept of the linear plots) and of the second-order rate constant for peroxynitrite isomerization by HSA-heme-Fe(III) (k_{on}; corresponding to the slope of the linear plots). In the presence of CO_2, values of k_0 for peroxynitrite isomerization in the absence of HSA-heme-Fe(III) (Table 1) are in good agreement with those obtained in the presence of HSA-heme-Fe(III)-CN and HSA (Fig. 2*D*) and reported in the literature (67, 70, 74).

Values of k_{on} for HSA-heme-Fe(III)-catalyzed isomerization of peroxynitrite are essentially unaffected by CO_2 (Table 1). In contrast, values of k_0 for peroxynitrite isomerization obtained in the presence of HSA-heme-Fe(III)-CN, HSA, and CO_2 are 10–100 times higher than those obtained in the absence of CO_2 (Table 1). The lack of a CO_2-linked effect on peroxynitrite isomerization by HSA-heme-Fe(III) is probably related to the fact that peroxynitrite reacts faster with HSA-heme-Fe(III) ($k_{on} = 4.1 \times 10^5$ and 4.5×10^5 M^{-1} s^{-1}, in the absence and presence of CO_2, respectively) (Table 1) than with CO_2 (the second-order rate constant being 3×10^4 M^{-1} s^{-1}) (74, 79).

To confirm the catalytic effect of HSA-heme-Fe(III) on peroxynitrite isomerization, the dependence of k_{obs} and k_0 on the peroxynitrite concentration was determined in the absence and presence of HSA-heme-Fe(III), HSA-heme-Fe(III)-CN, HSA, and CO_2 concentration, at pH 6.2 (data not shown), 7.2 (Fig. 3), and 8.1 (data not shown). Under all the experimental conditions, values of k_{obs} and k_0 for peroxynitrite isomerization slightly decrease upon increasing peroxynitrite concentration. In contrast, the amplitude of the kinetics increases as a function of the peroxynitrite concentration (data not shown). The decrease of k_{obs} and k_0 values upon increasing peroxynitrite concentration at fixed HSA-heme-Fe(III) concentration in the absence and presence of CO_2 (Fig. 3) is reminiscent of what has been reported for peroxynitrite isomerization by human Hb-Fe(III) and horse heart Mb-Fe(III) (70). This behavior has been proposed to reflect the occurrence of the peroxynitrite/peroxynitrous acid adduct at [peroxynitrite] $> 5.0 \times 10^{-5}$ M, around neutrality (70). Accordingly, the decrease of k_{obs} and k_0 values upon increasing the peroxynitrite concentration may reflect either the slow HSA-heme-Fe(III)-mediated decomposition of the peroxynitrite/peroxynitrous acid adduct or the slow dissociation of the peroxynitrite/peroxynitrous acid adduct preceding HSA-heme-Fe(III)-catalyzed peroxynitrite isomerization.

To highlight the role of the heme-Fe(III) atom to catalyze peroxynitrite isomerization, the effect of HSA-heme-Fe(III)-CN and HSA concentration on the isomerization of peroxynitrite was investigated in the absence and presence of CO_2. As shown in Fig. 2, *B* and *D*, HSA-heme-Fe(III)-CN and HSA do not affect the peroxynitrite isomerization kinetics. Therefore,

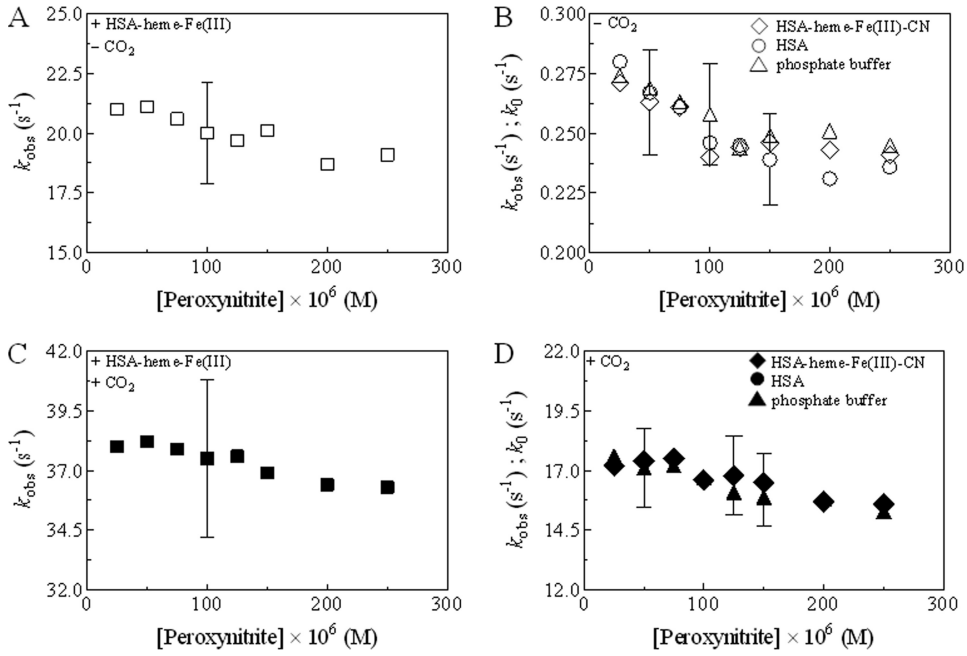

FIGURE 3. **Effect of peroxynitrite concentration on values of the (pseudo-)first-order rate constant for peroxynitrite isomerization in the presence of HSA-heme-Fe(III) (k_{obs}; *A* and *C*), HSA-heme-Fe(III)-CN (k_{obs}; *B* and *D*), HSA (k_{obs}; *B* and *D*), and 1.0×10^{-1} M phosphate buffer (k_0; *B* and *D*) in the absence (*A* and *B*) or presence (*C* and *D*) of CO_2, at pH 7.2 and 22.0 °C.** The HSA-heme-Fe(III), HSA-heme-Fe(III)-CN, and HSA concentrations were 5.0×10^{-6} M. The CO_2 concentration was 1.2×10^{-3} M. For clarity, the S.D. value was shown for prototypical k_{obs} and k_0 values in each *panel*.

the acceleration of the peroxynitrite isomerization rate by HSA-heme-Fe(III) could be due to the reaction of peroxynitrite with the heme-Fe(III) atom, as reported for human Hb-Fe(III) and horse heart Mb-Fe(III) (70).

The pH dependence of k_0 and k_{on} for peroxynitrite isomerization, in the absence and presence of HSA-heme-Fe(III) and CO_2, was examined to identify tentatively the species that preferentially react(s) with HSA-heme-Fe(III). Values of k_0 and k_{on} shown in Fig. 4 were derived from data reported in Fig. 2, *A* and *C*, and are listed in Table 1. Values of k_0 for peroxynitrite isomerization in the absence of HSA-heme-Fe(III) and CO_2 decrease upon increasing pH from 6.2 to 8.1 (Fig. 4*A*). In contrast, values of k_0 for peroxynitrite isomerization in the absence of HSA-heme-Fe(III) but in the presence of CO_2 increase upon raising the pH from 6.2 to 8.1 (Fig. 4*B*). In the absence and presence of CO_2, the pH dependence of k_{on} values for HSA-heme-Fe(III)-mediated isomerization of peroxynitrite (Fig. 4*C*) is closely similar to that of k_0 for peroxynitrite isomerization in the absence of HSA-heme-Fe(III) and CO_2 (Fig. 4*A*). The analysis of data reported in Fig. 4, according to Equations 4 and 5, allowed the estimation of pK_a values for the pH dependence of k_0 and k_{on} values for peroxynitrite isomerization in the absence and presence of HSA-heme-Fe(III) and CO_2.

The pH dependence of k_0 for peroxynitrite isomerization in the absence of both HSA-heme-Fe(III) and CO_2 ($pK_a = 6.8$) (Fig. 4*A*) and of k_{on} for peroxynitrite isomerization by HSA-heme-Fe(III) in the absence and presence of CO_2 ($pK_a = 6.9$) (Fig. 4*C*) is similar. The pK_a value (6.8) for the pH dependence of k_0 for peroxynitrite isomerization in the absence of both HSA-heme-Fe(III) and CO_2 here determined is in excellent agreement with pK_a values reported in the literature (74). In contrast, the pH dependence of k_0 for peroxynitrite isomerization in the absence of HSA-heme-Fe(III) but in the presence of CO_2 ($pK_a = 7.6$) (Fig. 4*B*) is different from that of k_0 for peroxynitrite isomerization in the absence of both HSA-heme-Fe(III) and CO_2 ($pK_a = 6.8$) (Fig. 4*A*) and of k_{on} for peroxynitrite isomerization by HSA-heme-Fe(III) in the absence and presence of CO_2 ($pK_a = 6.9$) (Fig. 4*C*).

According to the literature (67, 70), the close similarity of the pH dependence of k_0 for peroxynitrite isomerization in the absence of both HSA-heme-Fe(III) and CO_2 ($pK_a = 6.8$) (Fig. 4*A*) and of k_{on} for peroxynitrite isomerization by HSA-heme-Fe(III) in the absence and presence of CO_2 ($pK_a = 6.9$) (Fig. 4*C*) suggests that in all cases, HOONO is the species that reacts preferentially with the heme-Fe(III) atom. Conversely, the different pK_a value observed for peroxynitrite isomerization in the presence of CO_2 and in the absence of HSA-heme-Fe(III) ($pK_a = 7.6$) (Fig. 4*B*) could indicate that the species undergoing the isomerization is a transient highly reactive intermediate(s) formed by the reaction of peroxynitrite with CO_2. Since peroxynitrite has been reported to react with CO_2, leading to the formation of an adduct whose composition is believed to be $ONOOC(O)O^-$ (named 1-carboxylato-2-nitrosodioxidane) (74, 79), this might be the transient species that then converts to NO_3^- and CO_2 either directly or by transient formation of trioxocarbonate(•1-) ($CO_3^{\bullet-}$) and $^{\bullet}NO_2$. On the other hand, the similar pK_a values for peroxynitrite isomerization by HSA-heme-Fe(III), both in the absence and in the presence of CO_2 ($pK_a = 6.9$), indicates that peroxynitrite reacts with HSA-heme-Fe(III) as HOONO.

Ibuprofen Impairs HSA-Heme-Fe(III)-mediated Isomerization of Peroxynitrite—In the absence and presence of CO_2, ibuprofen impairs dose-dependently HSA-heme-Fe(III)-mediated isomerization of peroxynitrite (Fig. 5). Mixing HSA-heme-Fe(III) with peroxynitrite, in the presence of ibuprofen and in the absence and presence of CO_2, brings about a decrease of the absorbance at 302 nm (supplemental Fig. S2, *A* and *B*). Moreover, the kinetics of peroxynitrite isomerization by HSA-heme-Fe(III), in the presence of ibuprofen and in the absence and presence of CO_2, was fitted to a single-exponential decay for more than 97% of its course (supplemental Fig. S2, *A* and *B*). These findings agree with the results concerning peroxynitrite isomerization in the absence of ibuprofen (see above and supplemental Fig. S1).

The observed rate constant for HSA-heme-Fe(III)-catalyzed isomerization of peroxynitrite (k^i_{obs}) increases linearly with the HSA-heme-Fe(III) concentration over the whole ibuprofen concentration range explored, in the absence and presence of

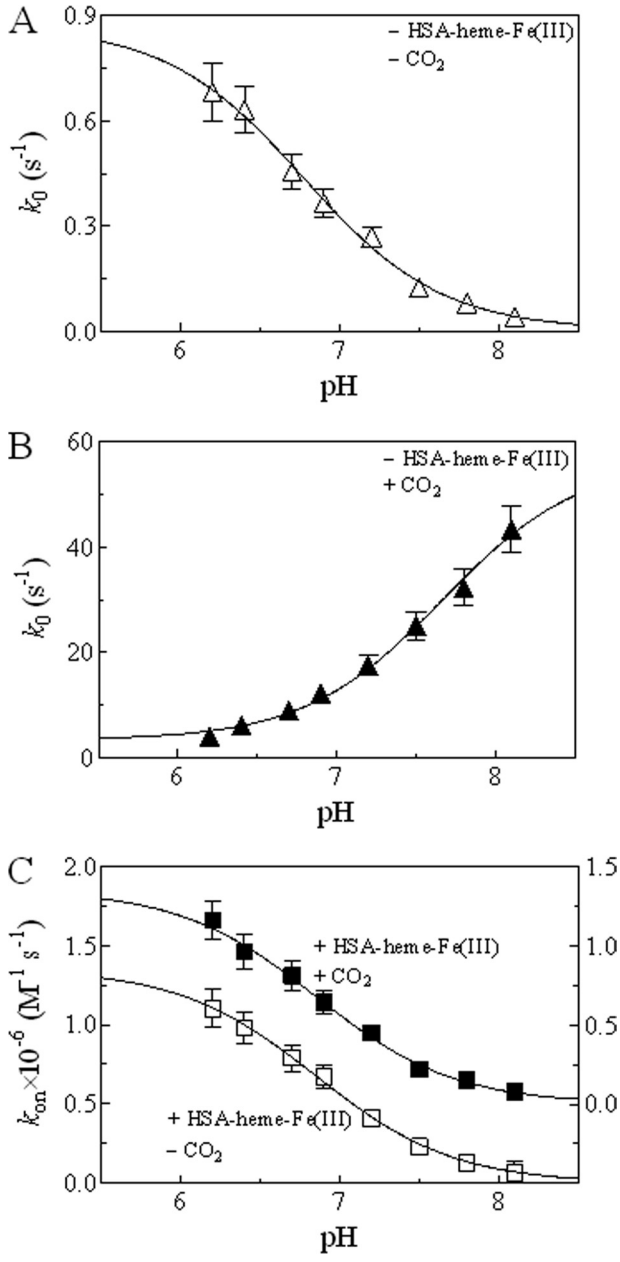

FIGURE 4. **Effect of pH on the first-order rate constant for peroxynitrite isomerization (k_0) in the absence (*A*) and presence (*B*) of CO_2 and on the second-order rate constant for HSA-heme-Fe(III)-mediated peroxynitrite isomerization (k_{on}) in the absence (*left*) and presence (*right*) of CO_2 (*C*), at 22.0 °C.** Values of k_0 in *A* and *B* are the average of those obtained from experiments of peroxynitrite isomerization in the absence and presence of HSA-heme-Fe(III) (see Table 1). The peroxynitrite concentration was 2.5×10^{-4} M. The CO_2 concentration was 1.2×10^{-3} M. The *continuous line* in *A* was calculated according to Equation 4 with $pK_a = 6.8$ and $k_{lim(top)} = 0.86\ s^{-1}$. The *continuous line* in *B* was calculated according to Equation 5 with $pK_a = 7.6$, $k_{lim(top)} = 55.3\ s^{-1}$, and $k_{lim(bottom)} = 3.1\ s^{-1}$. Both *continuous lines* in *C* were calculated according to Equation 4 with $pK_a = 6.9$ and $k_{lim(top)} = 1.4 \times 10^6\ M^{-1}\ s^{-1}$. Where not shown, the S.D. value is smaller than the *symbol*.

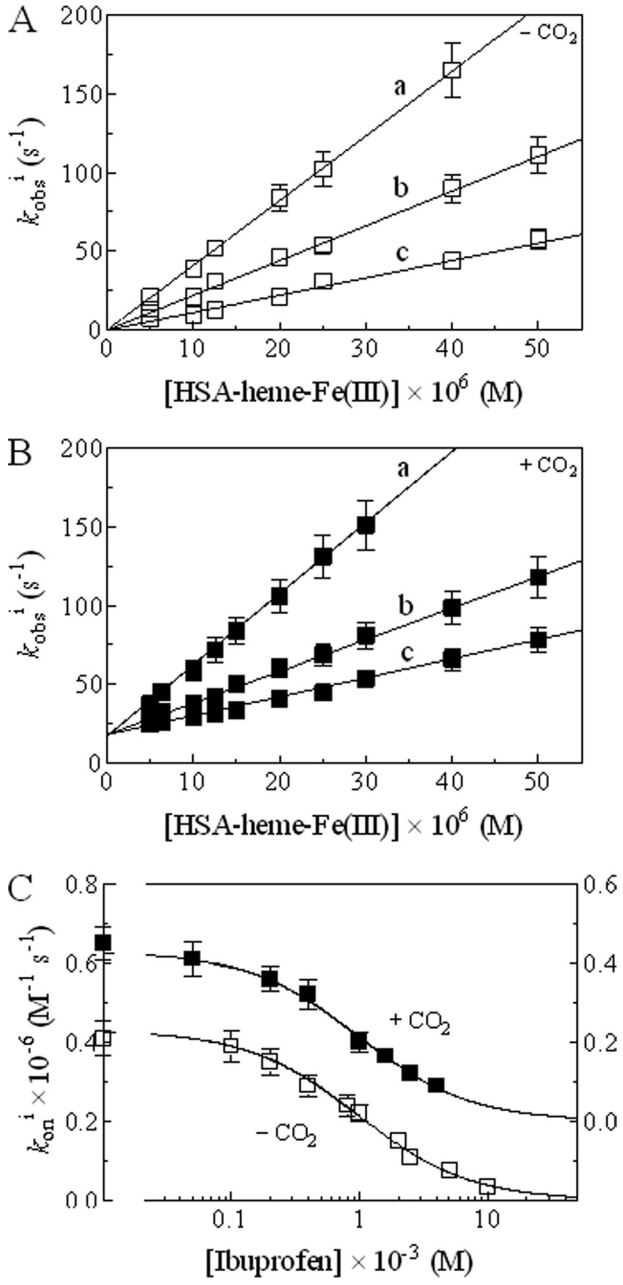

FIGURE 5. **Effect of the ibuprofen concentration on the dependence of the pseudo-first-order rate constant for peroxynitrite isomerization (k_{obs}^{i}) on the HSA-heme-Fe(III) concentration, in the absence (*A*) and presence (*B*) of CO_2, at pH 7.2 and 22.0 °C.** Data reported in panels *A* and *B* were obtained at [ibuprofen] = 0.0 M (*a*), 1.0×10^{-3} M (*b*), and 2.5×10^{-3} M (*c*). The *continuous lines* in *A* and *B* were calculated according to Equation 3 with values of k_{on}^{i} and k_0^{i} given in Table 2. Shown is the effect of the ibuprofen concentration on the second-order rate constant for HSA-heme(III)-catalyzed isomerization of peroxynitrite (k_{on}^{i}) in the absence (*left*) and presence (*right*) of CO_2 (*C*). Both continuous lines were calculated according to Equation 4 with $L = 9.7 \times 10^{-4}$ M and $k_{on(top)}^{i} = 4.3 \times 10^5\ M^{-1}\ s^{-1}$. Where not shown, the S.D. value is smaller than the *symbol*.

CO_2. The analysis of data reported in Fig. 5, *A* and *B*, according to Equation 3, allowed the determination of values of the first-order rate constant for peroxynitrite isomerization in the absence of HSA-heme-Fe(III) (k_0^{i}; corresponding to the *y* intercept of the linear plots) and of the second-order rate constant for peroxynitrite isomerization by HSA-heme(III) (k_{on}^{i}; corresponding to the slope of the linear plots) in the presence of ibuprofen and in the absence and presence of CO_2. As shown in Table 2, CO_2 does not affect k_{on}^{i} values but alters k_0^{i} values.

The effect of ibuprofen concentration on k_{on}^{i} values for HSA-heme-Fe(III)-mediated isomerization of peroxynitrite is shown in Fig. 5*C*. Values of k_0^{i} and k_{on}^{i} shown in Fig. 5*C* were derived from data reported in Fig. 5, *A* and *B*, and are listed in Table 2. Values of k_0^{i} are unaffected by ibuprofen concentration

TABLE 2
Effect of the ibuprofen concentration on k_0^i and k_{on}^i values for HSA-heme-Fe(III)-mediated peroxynitrite isomerization in the absence and presence of CO_2, at pH 7.2 and 22.0 °C

[Ibuprofen]	k_0^i		k_{on}^i	
	Without CO_2	With CO_2	Without CO_2	With CO_2
M	s^{-1}		$M^{-1}\ s^{-1}$	
0.0[a]	0.26[a]	17.8[a]	4.1×10^5 [a]	4.5×10^5 [a]
5.0×10^{-5}	ND[b]	19.3	ND	4.1×10^5
1.0×10^{-4}	0.23	ND	3.9×10^5	ND
2.0×10^{-4}	0.28	18.1	3.5×10^5	3.6×10^5
4.0×10^{-4}	0.25	17.6	2.9×10^5	3.2×10^5
8.0×10^{-4}	0.22	ND	2.4×10^5	ND
1.0×10^{-3}	0.24	18.4	2.2×10^5	2.0×10^5
1.6×10^{-3}	ND	19.0	ND	1.7×10^5
2.0×10^{-3}	0.26	ND	1.5×10^5	ND
2.5×10^{-3}	0.25	18.4	1.1×10^5	1.2×10^5
4.0×10^{-3}	ND	16.9	ND	9.0×10^4
5.0×10^{-3}	0.27	ND	7.5×10^4	ND
1.0×10^{-2}	0.22	ND	3.5×10^4	ND

[a] Under conditions where [ibuprofen] = 0.0 M, $k_0^i = k_0$, and $k_{on}^i = k_{on}$.
[b] ND, not determined.

(Table 2). In contrast, values of k_{on}^i for HSA-heme(III)-catalyzed isomerization of peroxynitrite decrease from 4.1×10^5 $M^{-1}\ s^{-1}$ in the absence of ibuprofen to 3.5×10^4 $M^{-1}\ s^{-1}$ at [ibuprofen] = 1.0×10^{-2} M in the absence of CO_2 and from 4.5×10^5 $M^{-1}\ s^{-1}$ in the absence of ibuprofen to 9.0×10^4 $M^{-1}\ s^{-1}$ at [ibuprofen] = 4.0×10^{-3} M in the presence of CO_2 (Table 2). The analysis of the dependence of k_{on}^i for HSA-heme(III)-catalyzed isomerization of peroxynitrite, according to Equation 4, allowed the determination of the CO_2-independent value of the dissociation equilibrium constant for ibuprofen binding to HSA-heme-Fe(III) ($L = 9.7 \times 10^{-4}$ M).

Analysis of the Nitrogen-containing Products of Peroxynitrate Isomerization—According to the literature (70, 80), the spontaneous isomerization of peroxynitrite yielded 76 ± 4% NO_3^- and 23 ± 3% NO_2^-. In the presence of HSA-heme-Fe(III), the NO_3^- and NO_2^- yields increased (~90%) and decreased (~10%), respectively, as reported for peroxynitrite isomerization catalyzed by human Hb-Fe(III) and horse heart Mb-Fe(III) (70). The same result has been observed in the presence of HSA-heme-Fe(III) and/or CO_2, according to the literature (70, 80). Last, ibuprofen does not significantly affect the NO_3^- and NO_2^- yields (supplemental Table S1).

Ibuprofen Impairs HSA-Heme-Fe(III)-based Protection of Free L-Tyrosine against Peroxynitrite-mediated Nitration—To investigate the protective role of HSA-heme-Fe(III) against peroxynitrite-mediated nitration, the relative yield of nitro-L-tyrosine formed by the reaction of peroxynitrite with free L-tyrosine in the presence of HSA-heme-Fe(III) was determined. For this purpose, 0.2 ml of a peroxynitrite solution were mixed with a free L-tyrosine solution, in the absence and presence of HSA-heme-Fe(III), HSA-heme-Fe(III)-CN, HSA, ibuprofen, and CO_2, as previously reported (67, 70). Note that CO_2 facilitates peroxynitrite-mediated nitration of L-tyrosine, redirecting peroxynitrite specificity (69, 74, 79).

As shown in Fig. 6, HSA-heme-Fe(III) protects dose-dependently free L-tyrosine against peroxynitrite-mediated nitration. In contrast, L-tyrosine nitration is not prevented by HSA-heme-Fe(III)-CN and HSA, and the relative nitro-L-tyrosine yield corresponds to that observed in the absence of HSA derivatives. According to previous results (67, 70), HSA-heme-Fe(III) was

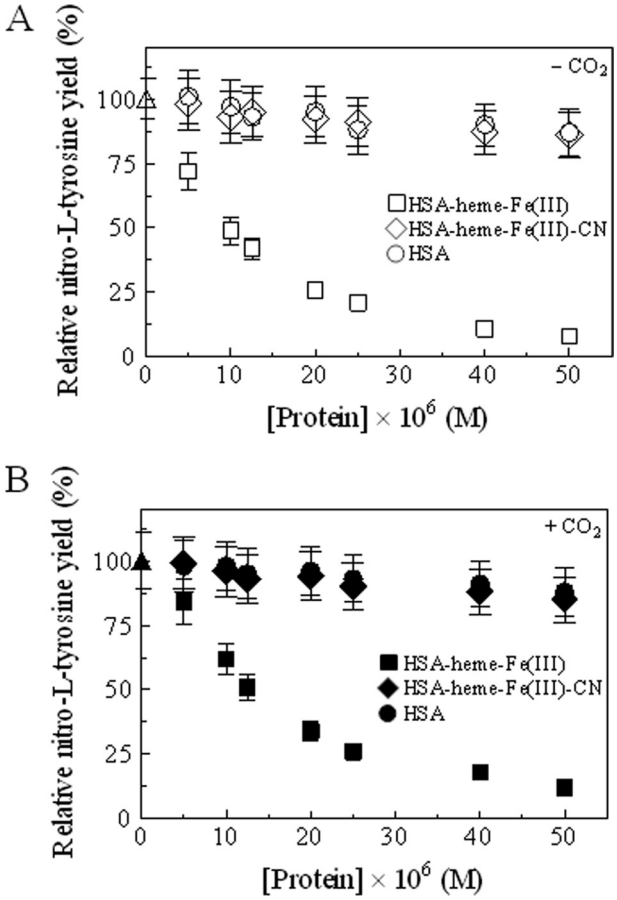

FIGURE 6. **Effect of HSA-heme-Fe(III), HSA-heme-Fe(III)-CN, and HSA concentration on the relative yield of nitro-L-tyrosine formed from the reaction of peroxynitrite with free L-tyrosine, at pH 7.2 and 22.0 °C, in the absence (*A*) and presence (*B*) of CO_2.** The free L-tyrosine concentration was 1.0×10^{-4} M. The peroxynitrite and CO_2 concentration was 2.0×10^{-4} and 1.2×10^{-3} M, respectively. Relative yield (%) = (yield with added protein/yield with no protein) × 100. Where not shown, the S.D. value is smaller than the *symbol*.

slightly less efficient at preventing peroxynitrite-mediated nitration of free L-tyrosine in the presence than in the absence of CO_2.

The ability of ibuprofen to impair allosterically HSA-heme-Fe(III)-mediated peroxynitrite isomerization prompted us to investigate the role of this drug in modulating peroxynitrite-based L-tyrosine nitration, in the absence and presence of CO_2. The relative yield of nitro-L-tyrosine increased upon increasing the ibuprofen concentration, at fixed HSA-heme-Fe(III), peroxynitrite, L-tyrosine, and CO_2 concentration (Fig. 7). The analysis of the data, according to Equation 7, allowed the determination of values of the dissociation equilibrium constant L in the absence and presence of CO_2 (8.7×10^{-4} and 8.4×10^{-4} M, respectively).

Spectrophotometric Evidence for Ibuprofen Binding to HSA-Heme-Fe(III)—To further support ibuprofen binding to HSA-heme-Fe(III), the value of the dissociation equilibrium constant for complex formation (L) has been determined spectrophotometrically (Fig. 8). The analysis of the data, according to Equation 6, allowed the determination of the dissociation equilibrium constant L (7.7×10^{-4} M). The value of L obtained spectrophotometrically (7.7×10^{-4} M) (Fig. 8) is in excellent

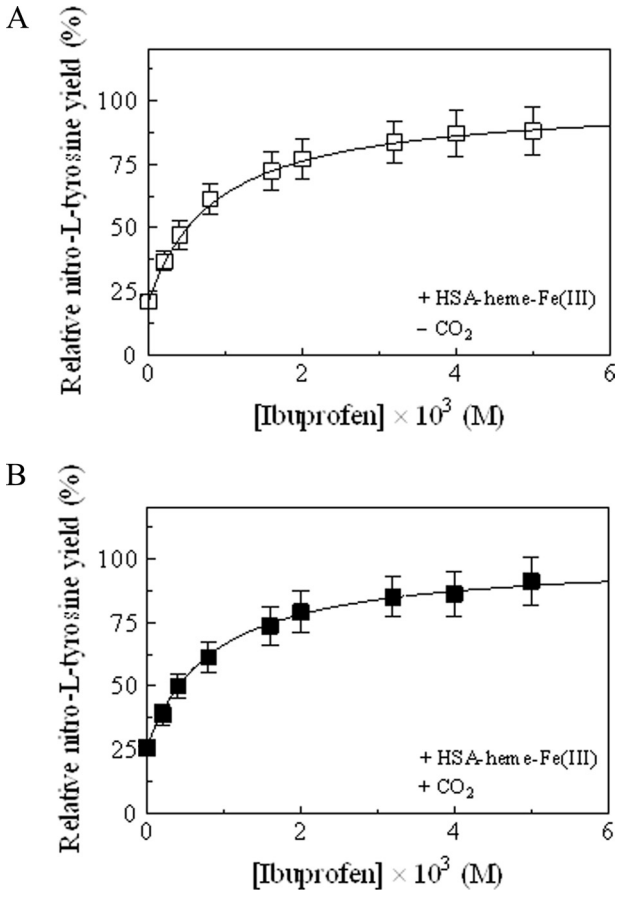

FIGURE 7. **Effect of ibuprofen concentration on the relative yield of nitro-L-tyrosine formed from the reaction of peroxynitrite with free L-tyrosine, at pH 7.2 and 22.0 °C, in the presence of HSA-heme-Fe(III) and in the absence (*A*) and presence (*B*) of CO_2.** The *continuous lines* were calculated according to Equation 7 with the following parameters: $L = 8.7 \times 10^{-4}$ M and $r = 21.1\%$ (*A*) and $L = 8.4 \times 10^{-4}$ M and $r = 25.9\%$ (*B*). The concentration of HSA-heme-Fe(III), peroxynitrite, free L-tyrosine, and CO_2 was 2.5×10^{-5}, 2.0×10^{-3}, 1.0×10^{-4}, and 1.2×10^{-3} M, respectively. Relative yield (%) = (yield with added protein/yield with no protein) × 100. Where not shown, the S.D. value is smaller than the *symbol*.

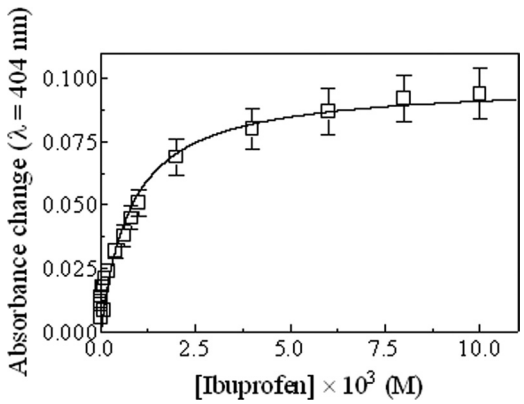

FIGURE 8. **Spectrophotometric titration of ibuprofen binding to HSA-heme-Fe(III), at pH 7.2 and 22.0 °C.** The HSA-heme-Fe(III) concentration was 1.0×10^{-5} M. The *continuous line* was calculated according to Equation 8 with $L = 7.7 \times 10^{-4}$ M. Where not shown, the S.D. value is smaller than the *symbol*.

agreement with those obtained from the effect of ibuprofen concentration on (i) HSA-heme-Fe(III)-catalyzed isomerization of peroxynitrite in the absence and presence of CO_2 ($L = 9.7 \times 10^{-4}$ M) (Fig. 5*C*) and (ii) the relative nitro-L-tyrosine yield in the absence and presence of CO_2 ($L = 8.7 \times 10^{-4}$ and 8.4×10^{-4} M, respectively) (Fig. 7). Note that the heme-Fe(III)-ibuprofen complex, which could potentially interfere, only occurs at an ibuprofen concentration of $\geq 7.5 \times 10^{-2}$ (38).

DISCUSSION

Ibuprofen, the prototype ligand of Sudlow's site II (1, 3, 26, 58), modulates allosterically peroxynitrite isomerization by HSA-heme-Fe(III) and therefore the peroxynitrite-mediated nitration of free L-tyrosine, highlighting the role of heterotropic ligands on the HSA reactivity (11, 13, 52, 81).

Peroxynitrite isomerization is facilitated by the HSA-heme-Fe(III) species, whereas the HSA-heme-Fe(III)-CN derivative and the heme-free HSA are both non-reactive, clearly demonstrating that the efficiency of the isomerization process mirrors the heme-Fe(III) reactivity. As already reported for horse and sperm whale Mb and human Hb (67, 70), peroxynitrous acid appears to be the species that preferentially reacts with HSA-heme-Fe(III). In addition, like horse heart Mb, sperm whale Mb, and human Hb (67, 70), HSA-heme-Fe(III) protects free L-tyrosine from peroxynitrite-mediated nitration.

Allosteric inhibition of the HSA-heme-Fe(III)-mediated peroxynitrite isomerization by ibuprofen is related to drug-dependent structural changes occurring at the FA1 site (*i.e.* at the heme binding pocket). Indeed, UV-visible, resonance Raman, and electron paramagnetic resonance spectroscopies evidenced that the pentacoordinated heme-Fe(III) atom of HSA-heme-Fe(III), observed in the absence of ibuprofen, becomes hexacoordinated low spin upon ibuprofen binding (38). On the basis of the crystal structure of HSA-heme-Fe(III) (21), the His^{146} residue was suggested as the putative ligand able to coordinate to the heme-Fe(III) atom in the sixth position upon ibuprofen binding (38). In contrast, in both ibuprofen-free pentacoordinated and ibuprofen-bound hexacoordinated HSA-heme-Fe(III), the Tyr^{161} residue coordinates to the heme-Fe(III) atom in the fifth position (38). Therefore, the presence of a strong ligand (either the His^{146} residue or the exogenous cyanide ligand) at the sixth coordination position of the heme-Fe(III) atom inhibits peroxynitrite isomerization, thus rendering HSA-heme-Fe(III) non-reactive.

The identity of the ibuprofen binding pocket(s) (among the three possible ones, namely FA2, FA6, and Sudlow's site II) responsible for this allosteric effect is still unclear.

Structural and solution studies of ibuprofen binding to HSA have shown that the ibuprofen primary binding site (*i.e.* Sudlow's site II formed by FA3 and FA4 clefts) does not appear to be allosterically linked to the heme binding site (*i.e.* FA1) (30, 37, 38, 55), ruling out the possibility that Sudlow's site II is responsible for the effect of ibuprofen on peroxynitrite isomerization by HSA-heme-Fe(III).

An additional candidate might be the ibuprofen secondary site FA6, which modulates negatively heme-Fe(III) binding to FA1 (12, 37) and the affinity of the secondary drug binding cleft FA2 (34, 37, 38, 81). The FA6 site (located within domain II at the interface between subdomains IIA and IIB)

is in close structural and functional contact with Sudlow's site I (*i.e.* the warfarin binding site), which is allosterically linked to the heme binding cleft (*i.e.* FA1) (12, 37). However, since the dissociation equilibrium constant for ibuprofen binding to the FA6 site has been reported to fall in the 4.0×10^{-7} to 1.3×10^{-5} M range (depending on the absence and presence of allosteric effector(s)) (55), we can also rule out that the effect of ibuprofen on peroxynitrite isomerization is related to drug binding to the FA6 site. Indeed, the average value of the dissociation equilibrium constant for ibuprofen binding to HSA-heme-Fe(III) here determined (L) from the dependence of either k_{on} or the relative yield of nitro-L-tyrosine or spectrophotometric changes in the Soret band on the ibuprofen concentration is at least 50-fold higher (8.8×10^{-4} M) (Figs. 6–8).

As a whole, FA2, the only ligand binding site that provides contacts with different HSA subdomains (being located at the interface between subdomains IIA and IIB), could represent the ibuprofen secondary cleft functionally linked to the heme-Fe(III) atom reactivity (37). Thus, the average value of L (8.8×10^{-4} M) here determined (Figs. 6–8) could reflect ibuprofen binding to the FA2 site of HSA-heme-Fe(III). Noticeably, this L value is grossly similar to that obtained from the ibuprofen-dependent resonance Raman spectroscopic changes of HSA-heme-Fe(III), reflecting hexacoordination of the heme-Fe(III) atom ($L = 4.0 \times 10^{-4}$ M) (38).

Peroxynitrite isomerization by heme-Fe(III) proteins (*e.g.* HSA-heme-Fe(III)) could represent a physiological detoxification mechanism, protecting cells from reactive nitrogen and oxygen species (78). Note that values of k_{on} for peroxynitrite isomerization by HSA-heme-Fe(III) are higher by about 1 order of magnitude than those reported for ferric horse heart Mb, sperm whale Mb, human Hb, and heme-model compounds (67, 70, 82, 83) (supplemental Table S2). Moreover, peroxynitrite isomerization by HSA-heme-Fe(III) (supplemental Table S2) is faster than peroxynitrite scavenging by ferrous nitrosylated heme proteins, which appears to be strongly limited by (i) the dissociation of the transient heme-Fe(III)-NO and (ii) the reduction of the final heme-Fe(III) species to the heme-Fe(II) derivative (50). Remarkably, peroxynitrite isomerization by heme-Fe(III) proteins (*e.g.* HSA-heme-Fe(III)) does not require any redox cycle.

Due to the relevant physiological role of HSA in human plasma, several *in vivo* implications can be argued from the present results. Indeed, peroxynitrite isomerization by HSA-heme-Fe(III) could occur only in patients affected with a variety of severe hematologic diseases characterized by excessive intravascular hemolysis. Under these pathological conditions, the HSA-heme-Fe(III) plasmatic level increases from the physiological concentration ($\sim 1 \times 10^{-6}$ M) to $\sim 4 \times 10^{-5}$ M (59, 84), HSA acting as the main heme-Fe(III) plasma depot (84, 85). To mimic as much as possible this condition, the HSA-heme-Fe(III) concentration here used ranged from 5.0×10^{-6} to 5.0×10^{-5} M. The high heme plasma concentration is invariably associated with a reduction of hemopexin in patients affected by excessive intravascular hemolysis (59). Note that upon increasing heme plasma level, hemopexin, whose plasma concentration ($\sim 1.5 \times 10^{-5}$ M) (84, 85) is about 2 orders of magnitude lower than that of HSA (7.5×10^{-4} M) (3), undergoes heme saturation, highlighting the role of HSA as a heme scavenger (84, 85).

Although the *in vivo* concentration of peroxynitrite is openly debated, the level of peroxynitrite in the reperfused ischemic heart has been reported to be much higher than micromolar concentration, at least over brief period of time (86, 87), overlapping with the lowest peroxynitrite concentration here used (2.5×10^{-5} M).

Finally, considering the plasma level of ibuprofen ($\sim 10^{-4}$ to 10^{-3} M) (88–90), the drug concentration here used ranged between 5.0×10^{-5} M and 1.0×10^{-2} M. Accounting for the average L value ($\sim 8.8 \times 10^{-4}$ M) here determined and the plasma level of ibuprofen, the molar fraction of the drug-bound HSA-heme-Fe(III) could range between 10 and 50%.

CONCLUSIONS

Data here reported highlight the role of drugs in modulating HSA functions. This is relevant for the potential role played by HSA-heme in the detoxification process, also taking into account that the HSA-heme-Fe(III) plasmatic concentration increases significantly under pathological conditions (11, 13, 52, 59, 84). Therefore, the higher HSA-heme concentration and the higher efficiency of peroxynitrite isomerization altogether contribute to identify HSA-heme as a major detoxification element in the bloodstream. This aspect acquires an even higher value in consideration of the protective role, played by the peroxynitrite isomerization, on the nitration of aromatic residues (such as tyrosine), which represent a relevant post-translational protein modification process (91). Last, HSA, not only acting as a heme carrier but also displaying transient heme-based properties, represents a case for "chronosteric effects" (52), which opens the scenario toward the possibility of a time- and metabolite-dependent multiplicity of roles for HSA.

Acknowledgment—We thank Dr. Elisabetta De Marinis for helpful discussions.

REFERENCES

1. Sudlow, G., Birkett, D. J., and Wade, D. N. (1975) *Mol. Pharmacol.* **11,** 824–832
2. Carter, D. C., and Ho, J. X. (1994) *Adv. Protein Chem.* **45,** 153–203
3. Peters, T., Jr. (1996) *All about Albumin: Biochemistry, Genetics and Medical Applications*, Academic Press, Inc., San Diego
4. Bertucci, C., and Domenici, E. (2002) *Curr. Med. Chem.* **9,** 1463–1481
5. Curry, S. (2002) *Vox Sang.* **83,** Suppl. 1, 315–319
6. Kragh-Hansen, U., Chuang, V. T., and Otagiri, M. (2002) *Biol. Pharm. Bull.* **25,** 695–704
7. Sakurai, Y., Ma, S. F., Watanabe, H., Yamaotsu, N., Hirono, S., Kurono, Y., Kragh-Hansen, U., and Otagiri, M. (2004) *Pharm. Res.* **21,** 285–292
8. Sułkowska, A., Bojko, B., Równicka, J., and Sułkowski, W. (2004) *Biopolymers* **74,** 256–262
9. Ascenzi, P., Bocedi, A., Bolli, A., Fasano, M., Notari, S., and Polticelli, F. (2005) *Biochem. Mol. Biol. Educ.* **33,** 169–176
10. Bocedi, A., Notari, S., Menegatti, E., Fanali, G., Fasano, M., and Ascenzi, P. (2005) *FEBS J.* **272,** 6287–6296
11. Fasano, M., Curry, S., Terreno, E., Galliano, M., Fanali, G., Narciso, P., Notari, S., and Ascenzi, P. (2005) *IUBMB Life* **57,** 787–796
12. Ghuman, J., Zunszain, P. A., Petitpas, I., Bhattacharya, A. A., Otagiri, M., and Curry, S. (2005) *J. Mol. Biol.* **353,** 38–52

13. Ascenzi, P., Bocedi, A., Notari, S., Fanali, G., Fesce, R., and Fasano, M. (2006) *Mini Rev. Med. Chem.* **6,** 483–489
14. Zunszain, P. A., Ghuman, J., McDonagh, A. F., and Curry, S. (2008) *J. Mol. Biol.* **381,** 394–406
15. He, X. M., and Carter, D. C. (1992) *Nature* **358,** 209–215
16. Curry, S., Mandelkow, H., Brick, P., and Franks, N. (1998) *Nat. Struct. Biol.* **5,** 827–835
17. Sugio, S., Kashima, A., Mochizuki, S., Noda, M., and Kobayashi, K. (1999) *Protein Eng.* **12,** 439–446
18. Bhattacharya, A. A., Curry, S., and Franks, N. P. (2000) *J. Biol. Chem.* **275,** 38731–38738
19. Bhattacharya, A. A., Grüne, T., and Curry, S. (2000) *J. Mol. Biol.* **303,** 721–732
20. Petitpas, I., Bhattacharya, A. A., Twine, S., East, M., and Curry, S. (2001) *J. Biol. Chem.* **276,** 22804–22809
21. Wardell, M., Wang, Z., Ho, J. X., Robert, J., Ruker, F., Ruble, J., and Carter, D. C. (2002) *Biochem. Biophys. Res. Commun.* **291,** 813–819
22. Petitpas, I., Petersen, C. E., Ha, C. E., Bhattacharya, A. A., Zunszain, P. A., Ghuman, J., Bhagavan, N. V., and Curry, S. (2003) *Proc. Natl. Acad. Sci. U.S.A.* **100,** 6440–6445
23. Zunszain, P. A., Ghuman, J., Komatsu, T., Tsuchida, E., and Curry, S. (2003) *BMC Struct. Biol.* **3,** 6
24. Simard, J. R., Zunszain, P. A., Hamilton, J. A., and Curry, S. (2006) *J. Mol. Biol.* **361,** 336–351
25. Fasano, M., Fanali, G., Leboffe, L., and Ascenzi, P. (2007) *IUBMB Life* **59,** 436–440
26. Sudlow, G., Birkett, D. J., and Wade, D. N. (1976) *Mol. Pharmacol.* **12,** 1052–1061
27. Diana, F. J., Veronich, K., and Kapoor, A. L. (1989) *J. Pharm. Sci.* **78,** 195–199
28. Yamasaki, K., Maruyama, T., Yoshimoto, K., Tsutsumi, Y., Narazaki, R., Fukuhara, A., Kragh-Hansen, U., and Otagiri, M. (1999) *Biochim. Biophys. Acta* **1432,** 313–323
29. Dockal, M., Chang, M., Carter, D. C., and Rüker, F. (2000) *Protein Sci.* **9,** 1455–1465
30. Baroni, S., Mattu, M., Vannini, A., Cipollone, R., Aime, S., Ascenzi, P., and Fasano, M. (2001) *Eur. J. Biochem.* **268,** 6214–6220
31. Simard, J. R., Zunszain, P. A., Ha C. E., Yang, J. S., Bhagavan, N. V., Petitpas, I., Curry, S., and Hamilton, J. A. (2005) *Proc. Natl. Acad. Sci. U.S.A.* **102,** 17958–17963
32. Spector, A. A. (1975) *J. Lipid Res.* **16,** 165–179
33. Hamilton, J. A., Cistola, D. P., Morrisett, J. D., Sparrow, J. T., and Small, D. M. (1984) *Proc. Natl. Acad. Sci. U.S.A.* **81,** 3718–3722
34. Chuang, V. T., and Otagiri, M. (2002) *Pharm. Res.* **19,** 1458–1464
35. Hamilton, J. A. (2004) *Prog. Lipid Res.* **43,** 177–199
36. Fasano, M., Baroni, S., Vannini, A., Ascenzi, P., and Aime, S. (2001) *J. Biol. Inorg. Chem.* **6,** 650–658
37. Fanali, G., Bocedi, A., Ascenzi, P., and Fasano, M. (2007) *FEBS J.* **274,** 4491–4502
38. Nicoletti, F. P., Howes, B. D., Fittipaldi, M., Fanali, G., Fasano, M., Ascenzi, P., and Smulevich, G. (2008) *J. Am. Chem. Soc.* **130,** 11677–11688
39. Dill, K. A., Alonso, D. O., and Hutchinson, K. (1989) *Biochemistry* **28,** 5439–5449
40. Carter, D. C., Ho, J. X., and Rüker, F. (September 7, 1999) United States Patent 5,948,609
41. Komatsu, T., Matsukawa, Y., and Tsuchida, E. (2000) *Bioconjug. Chem.* **11,** 772–776
42. Mattu, M., Vannin, A., Coletta, M., Fasano, M., and Ascenzi, P. (2001) *J. Inorg. Biochem.* **84,** 293–296
43. Monzani, E., Bonafè, B., Fallarini, A., Redaelli, C., Casella, L., Minchiotti, L., and Galliano, M. (2001) *Biochim. Biophys. Acta* **1547,** 302–312
44. Fasano, M., Mattu, M., Coletta, M., and Ascenzi, P. (2002) *J. Inorg. Biochem.* **91,** 487–490
45. Kamal, J. K., and Behere, D. V. (2002) *J. Biol. Inorg. Chem.* **7,** 273–283
46. Monzani, E., Curto, M., Galliano, M., Minchiotti, L., Aime, S., Baroni, S., Fasano, M., Amoresano, A., Salzano, A. M., Pucci, P., and Casella, L. (2002) *Biophys. J.* **83,** 2248–2258
47. Komatsu, T., Ohmichi, N., Zunszain, P. A., Curry, S., and Tsuchida, E. (2004) *J. Am. Chem. Soc.* **126,** 14304–14305
48. Fanali, G., Fesce, R., Agrati, C., Ascenzi, P., and Fasano, M. (2005) *FEBS J.* **272,** 4672–4683
49. Komatsu, T., Ohmichi, N., Nakagawa, A., Zunszain, P. A., Curry, S., and Tsuchida, E. (2005) *J. Am. Chem. Soc.* **127,** 15933–15942
50. Ascenzi, P., and Fasano, M. (2007) *Biochem. Biophys. Res. Commun.* **353,** 469–474
51. Ascenzi, P., Imperi, F., Coletta, M., and Fasano, M. (2008) *Biochem. Biophys. Res. Commun.* **369,** 686–691
52. Fasano, M., Fanali, G., Fesce, R., and Ascenzi, P. (2008) *Human Serum Haeme-albumin: An Allosteric "Chronosteric" Protein*, pp. 121–131, Springer, Heidelberg
53. Baroni, S., Pariani, G., Fanali, G., Longo, D., Ascenzi, P., Aime, S., and Fasano, M. (2009) *Biochem. Biophys. Res. Commun.* **385,** 385–389
54. Fanali, G., De Sanctis, G., Gioia, M., Coletta, M., Ascenzi, P., and Fasano, M. (2009) *J. Biol. Inorg. Chem.* **14,** 209–217
55. Fanali, G., Pariani, G., Ascenzi, P., and Fasano, M. (2009) *FEBS J.* **276,** 2241–2250
56. Kragh-Hansen, U., Watanabe, H., Nakajou, K., Iwao, Y., and Otagiri, M. (2006) *J. Mol. Biol.* **363,** 702–712
57. Ascenzi, P., Bocedi, A., Notari, S., Menegatti, E., and Fasano, M. (2005) *Biochem. Biophys. Res. Commun.* **334,** 481–486
58. Bocedi, A., Notaril, S., Narciso, P., Bolli, A., Fasano, M., and Ascenzi, P. (2004) *IUBMB Life* **56,** 609–614
59. Muller-Eberhard, U., Javid, J., Liem, H. H., Hanstein, A., and Hanna, M. (1968) *Blood* **32,** 811–815
60. Kharitonov, V. G., Sharma, V. S., Magde, D., and Koesling, D. (1997) *Biochemistry* **36,** 6814–6818
61. Boffi, A., Das, T. K., della Longa, S., Spagnuolo, C., and Rousseau, D. L. (1999) *Biophys. J.* **77,** 1143–1149
62. Cabrera-Crespo, J., Gonçalves, V. M., Martins, E. A., Grellet, S., Lopes, A. P., and Raw, I. (2000) *Biotechnol. Appl. Biochem.* **31,** 101–106
63. Fasano, M., Bocedi, A., Mattu, M., Coletta, M., and Ascenzi, P. (2004) *J. Biol. Inorg. Chem.* **9,** 800–806
64. Bohle, D. S., Glassbrenner, P. A., and Hansert, B. (1996) *Methods Enzymol.* **269,** 302–311
65. Koppenol, W. H., Kissner, R., and Beckman, J. S. (1996) *Methods Enzymol.* **269,** 296–302
66. Herold, S., Exner, M., and Boccini, F. (2003) *Chem. Res. Toxicol.* **16,** 390–402
67. Herold, S., Kalinga, S., Matsui, T., and Watanabe, Y. (2004) *J. Am. Chem. Soc.* **126,** 6945–6955
68. Ascenzi, P., and Visca, P. (2008) *Methods Enzymol.* **436,** 317–337
69. Goldstein, S., and Merényi, G. (2008) *Methods Enzymol.* **436,** 49–61
70. Herold, S., and Shivashankar, K. (2003) *Biochemistry* **42,** 14036–14046
71. Antonini, E., and Brunori, M. (1971) *Hemoglobin and Myoglobin in Their Reactions with Ligands*, North-Holland, Amsterdam
72. Pfeiffer, S., Gorren, A. C., Schmidt, K., Werner, E. R., Hansert, B., Bohle, D. S., and Mayer, B. (1997) *J. Biol. Chem.* **272,** 3465–3470
73. Herold, S., Matsui, T., and Watanabe, Y. (2001) *J. Am. Chem. Soc.* **123,** 4085–4086
74. Goldstein, S., Lind, J., and Merényi, G. (2005) *Chem. Rev.* **105,** 2457–2470
75. Miranda, K. M., Espey, M. G., and Wink, D. A. (2001) *Nitric Oxide* **5,** 62–71
76. Ascenzi, P., Bocedi, A., Bolognesi, M., Fabozzi, G., Milani, M., and Visca, P. (2006) *Biochem. Biophys. Res. Commun.* **339,** 450–456
77. Squadrito, G. L., and Pryor, W. A. (2002) *Chem. Res. Toxicol.* **15,** 885–895
78. Herold, S., and Fago, A. (2005) *Comp. Biochem. Physiol. A Mol. Integr. Physiol.* **142,** 124–129
79. Ascenzi, P., Bocedi, A., Visca, P., Minetti, M., and Clementi, E. (2006) *IUBMB Life* **58,** 611–613
80. Kissner, R., and Koppenol, W. H. (2002) *J. Am. Chem. Soc.* **124,** 234–239
81. Ascenzi, P., di Masi, A., De Sanctis, G., Coletta, M., and Fasano, M. (2009) *Biochem. Biophys. Res. Commun.* **387,** 83–86
82. Groves, J. T. (1999) *Curr. Opin. Chem. Biol.* **3,** 226–235
83. Shimanovich, R., and Groves, J. T. (2001) *Arch. Biochem. Biophys.* **387,** 307–317
84. Miller, Y. I., and Shaklai, N. (1999) *Biochim. Biophys. Acta* **1454,**

153–164
85. Ascenzi, P., Bocedi, A., Visca, P., Altruda, F., Tolosano, E., Beringhelli, T., and Fasano, M. (2005) *IUBMB Life* **57,** 749–759
86. Schulz, R., Dodge, K. L., Lopaschuk, G. D., and Clanachan, A. S. (1997) *Am. J. Physiol.* **272,** H1212–H1219
87. Ma, X. L., Gao, F., Lopez, B. L., Christopher, T. A., and Vinten-Johansen, J. (2000) *J. Pharmacol. Exp. Ther.* **292,** 912–920
88. Regazzi, B. M., Rondanelli, R., Ciaroelli, L., Bartoli, A. L., and Rampini, A. (1986) *Int. J. Clin. Pharmacol. Res.* **6,** 469–473
89. Martin, W., Koselowske, G., Töberich, H., Kerkmann, T., Mangold, B., and Augustin, J. (1990) *Biopharm. Drug Dispos.* **11,** 265–278
90. Brown, R. D., Wilson, J. T., Kearns, G. L., Eichler, V. F., Johnson, V. A., and Bertrand, K. M. (1992) *J. Clin. Pharmacol.* **32,** 231–241
91. Alvarez, B., and Radi, R. (2003) *Amino Acids* **25,** 295–311

ADDITIONS AND CORRECTIONS

This paper is available online at www.jbc.org

THE JOURNAL OF BIOLOGICAL CHEMISTRY VOL. 286, NO. 33, p. 29441, August 19, 2011

VOLUME 282 (2007) PAGES 4288–4300
DOI 10.1074/jbc.A111.608307

Activation of JNK-dependent pathway is required for HIV Viral Protein R-induced apoptosis in human monocytic cells. *INVOLVEMENT OF ANTIAPOPTOTIC BCL2 AND c-IAP1 GENES*.

Sasmita Mishra, Jyoti P. Mishra, and Ashok Kumar

PAGE 4293:

Fig. 3*A* (*upper right panel*) shows an alteration of a lane (10 μM PD98059) that was not detected at the time of manuscript submission and that is contrary to the *Journal of Biological Chemistry* guidelines. Herein, we provide an alternative figure that shows that the ERK inhibitor PD98059 inhibited Vpr-(52–96)-induced ERK activation in a dose-dependent manner. THP-1 cells were treated with the indicated concentrations of PD98059 for 4 h, followed by stimulation with 1.5 μM Vpr-(52–96) peptide for another 2 h. The legend of this figure remains unchanged. The data support the published observations and therefore do not impact the interpretation of this figure or the central conclusion of this article.

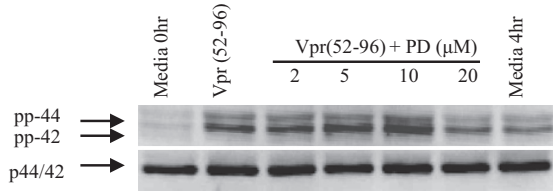

VOLUME 285 (2010) PAGES 21858–21867
DOI 10.1074/jbc.A110.117291

Nucleolar targeting of the chaperone Hsc70 is regulated by stress, cell signaling, and a composite targeting signal which is controlled by autoinhibition.

Piotr Bański, Hicham Mahboubi, Mohamed Kodiha, Sanhita Shrivastava, Cynthia Kanagaratham, and Ursula Stochaj

During the continuation of our work on hsc70 trafficking, we have noticed that there was an error during the preparation of midiprep plasmid DNA for two constructs that were described in this work. The error reported by us does not alter the validity of the raw data. The following two constructs were affected by the error: GFP-hsc70(225–262) and GFP-hsc70(245–287). These two plasmid DNAs have been inverted in our article. Following the detection of the error, we have verified the correctness of all other constructs encoding wild-type or mutant fragments of domain IIB of hsc70. This error affects the presentation of results shown in Figs. 2*B* and 3 (*A* and *C*) and the interpretation depicted in Fig. 6*A*. Thus, the correct interpretation of our data is that segment 245–287 locates constitutively in the nucleolus under non-stress and stress conditions. Fragment 225–262 displays weak stress-induced nucleolar accumulation. This makes residues 225–244 the negative regulator of hsc70 nucleolar accumulation.

VOLUME 284 (2009) PAGES 6079–6092
DOI 10.1074/jbc.A111.806077

Preparation and properties of asymmetric vesicles that mimic cell membranes. *EFFECT UPON LIPID RAFT FORMATION AND TRANSMEMBRANE HELIX ORIENTATION.*

Hui-Ting Cheng, Megha, and Erwin London

The experiments reported were carried out at 390 mM methyl-β-cyclodextrin (MβCD; 825 mg + 1 ml of water, which gives a volume of ~1.6 ml), not as reported at 625 mM MβCD (825 mg/ml of solution). We (MiJin Son and E. L.) have investigated asymmetric vesicle preparation at the higher MβCD concentration and found that 625 mM MβCD could be used to produce asymmetric small unilamellar vesicles. However, the results were not as reproducible as with the lower MβCD concentration. We recommend the use of 390 mM MβCD to prepare asymmetric small unilamellar vesicles.

VOLUME 284 (2009) PAGES 31006–31017
DOI 10.1074/jbc.A109.010736

Ibuprofen impairs allosterically peroxynitrite isomerization by ferric human serum heme-albumin.

Paolo Ascenzi, Alessandra di Masi, Massimo Coletta, Chiara Ciaccio, Gabriella Fanali, Francesco P. Nicoletti, Giulietta Smulevich, and Mauro Fasano

For graphical reasons, $k_{obs} = (k_{on} \times 10) \times [\text{HSA-heme-Fe(III)}] + k_0$ and $k^i_{obs} = (k^i_{on} \times 10) \times [\text{HSA-heme-Fe(III)}] + k^i_0$. Although the values of k_{on} and k^i_{on} are reported correctly in the text and in Tables 1 and 2, derivation from data reported in Figs. 2, 3, and 5 corresponds to $k_{on} \times 10$ and $k^i_{on} \times 10$.

VOLUME 285 (2010) PAGES 473–482
DOI 10.1074/jbc.A109.040238

YybT is a signaling protein that contains a cyclic dinucleotide phosphodiesterase domain and a GGDEF domain with ATPase activity.

Feng Rao, Rui Yin See, Dongwei Zhang, Delon Chengxu Toh, Qiang Ji, and Zhao-Xun Liang

PAGE 473:

The first sentence in the Abstract should read as follows: The cyclic dinucleotide c-di-AMP synthesized by the diadenylate cyclase domain was discovered recently as a messenger molecule for signaling DNA breaks in *Bacillus subtilis*.

In the Introduction, line 21 in the right-hand column should read as follows: This group of proteins (COG3887), as represented by the *B. subtilis* protein YybT, contains two N-terminal transmembrane helices, a region that shares minimum sequence homology with some Per-Arnt-Sim (PAS) domains, a highly modified GGDEF domain, and a DHH/DHHA1 domain (see Fig. 1).

We suggest that subscribers photocopy these corrections and insert the photocopies in the original publication at the location of the original article. Authors are urged to introduce these corrections into any reprints they distribute. Secondary (abstract) services are urged to carry notice of these corrections as prominently as they carried the original abstracts.

Ibuprofen Impairs Allosterically Peroxynitrite Isomerization by Ferric Human Serum Heme-Albumin

Paolo Ascenzi, Alessandra di Masi, Massimo Coletta, Chiara Ciaccio, Gabriella Fanali, Francesco P. Nicoletti, Giulietta Smulevich and Mauro Fasano

J. Biol. Chem. 2009, 284:31006-31017.
doi: 10.1074/jbc.M109.010736 originally published online September 3, 2009
